Significant Electronic Thermal Transport in the Conducting Polymer Poly(3,4-ethylenedioxythiophene)

Annie Weathers, Zia Ullah Khan, Robert Brooke, Drew Evans, Michael T. Pettes, Jens Wenzel Andreasen, Xavier Crispin and Li Shi

Original Publication:

Annie Weathers, Zia Ullah Khan, Robert Brooke, Drew Evans, Michael T. Pettes, Jens Wenzel Andreasen, Xavier Crispin and Li Shi, Significant Electronic Thermal Transport in the Conducting Polymer Poly(3,4-ethylenedioxythiophene), 2015, Advanced Materials, (27), 12, 2101-2106.
http://dx.doi.org/10.1002/adma.201404738

DOI: 10.1002/((please add manuscript number))
Article type: Communication

Significant electronic thermal transport in the conducting polymer poly(3,4-ethylenedioxythiophene) (PEDOT)

*Annie Weathers, Zia Ullah Khan, Robert Brooke, Drew Evans, Michael T. Pettes, Xavier Crispin, and Li Shi**

A. Weathers, Dr. M.T. Pettes, Prof. L. Shi
Department of Mechanical Engineering, The University of Texas at Austin, Austin, 78712,USA
E-mail: lishi@mail.utexas.edu

Z.U. Khan, Prof. X. Crispin
Linkoping University, Department of Science and Technology, Organic Electronics, SE-601 74 Norrkoping, Sweden

R. Brooke, Dr. D. Evans
Thin Film Coatings Group, Mawson Institute, University of South Australia, Mawson Lakes, 5095, Australia

Keywords: Conducting polymers, organic electronics, poly(3,4-ethylenedioxythiophene), thermoelectric, Wiedemann-Franz law, thermal conductivity

Conjugated polymers contain an unsaturated carbon backbone characterized by a delocalization of π- electrons along the polymer chain. The doping charges in conjugated polymers are polarons, which are fermionic quasiparticles composed of a charge and a geometrical distortion of the bonding. A pair of doping charges localized on the same geometrical defect is termed a bipolaron, which carries no net spin.[1] By oxidizing or reducing the polymer backbone, the system can be doped to p-type or n-type with a wide range of conductivities that span 10 orders of magnitude and depend on the material microstructure and processing conditions.[2] Such large variability enables a wealth of possibilities for their electronic applications. In addition, conducting polymers offer several key advantages over their inorganic counterparts, such as mechanical flexibility, transparency, and material abundance, which can enable low-cost fabrication and novel applications such as

printed and flexible electronics.[3] Therefore, since the development of conducting polymers in the 1970s,[4] there has been continuous advancement in their use for light emitting diodes,[5] transistors,[6] memory storage,[7] solar cells,[8] energy storage,[9] and more recently thermoelectric devices.[10]

While electronic transport properties are crucial to the function of organic devices, the performance and reliability of these devices are also influenced by the thermal properties. For electronic and many other applications, high thermal conductivity is necessary to provide efficient cooling of the current-carrying regions in the device. Indeed, this requirement has fueled a strong interest in understanding size dependent thermal transport in materials such as silicon and graphene for their use in electronic devices.[11] On the other hand, the energy efficiency of thermoelectric devices increases with increasing material figure of merit, $ZT = S^2\sigma T/\kappa$, where S is the Seebeck coefficient, σ is the electrical conductivity, κ is the thermal conductivity, and T is the absolute temperature, making low-thermal conductivity materials desirable for this application. The thermal conductivity consists of contributions from phonons, namely lattice vibrations, and electrons. The lattice thermal conductivity, κ_L, of conducting polymers is typically very low, even lower than typical values for highly disordered inorganic materials. This feature can present potential challenges in the use of conducting polymers for electronics, but has prompted interest in their use for thermoelectric conversion.

One prominent conducting polymer system is poly(3,4-ethylenedioxythiophene) (PEDOT), which has been studied recently as a leading organic thermoelectric material.[12, 13] Some early reports on the thermoelectric properties of PEDOT focused on bulk composites filled with carbon nanotubes[14, 15] and Bi_2Te_3[16], which benefit from an improved power factor, $S^2\sigma$, over bulk PEDOT.[17] A number of recent papers have reported a dramatic improvement in the thermoelectric properties of PEDOT thin films through engineering of the

doping chemistry. A room-temperature power factor of 300 $\mu Wm^{-1}K^{-2}$ has been shown in PEDOT:Tosylate films,[18] in comparison to 4770 $\mu Wm^{-1}K^{-2}$ for Bi_2Te_3.[19] In addition, PEDOT films prepared by vapor-phase polymerization show an electronic structure consistent with semi-metallic conduction, which results in an electrical conductivity as high as 2000 S/cm, just one order of magnitude lower than those of titanium or stainless steel. Interestingly, *S* was found to increase with increasing σ, which is an opposite trend to that for typical semiconductors.[13]

Recently, a room-temperature *ZT* value of 0.4 has been reported in PEDOT:polystyrene sulfonate (PSS), and is the highest value reported to date for an organic material.[12] This *ZT* value was calculated based on an in-plane σ value of 620 S/cm measured on a set of PEDOT:PSS thin film samples, and an in-plane κ of 0.42 $Wm^{-1}K^{-1}$ measured on another set of PEDOT:PSS thin film samples which required different processing steps for thermal conductivity measurements. The electronic contribution to κ for a typical metal can be well described by the Wiedemann-Franz law as $\kappa_e = (k_b/e)^2 L\sigma T$, [20] where k_b is the Boltzmann constant, e is the elemental charge, and L is the dimensionless Lorenz factor, which takes the theoretical Sommerfeld value of $L_0 = \pi^2/3$ for a degenerate Fermi gas such as electrons in a metal. If L is assumed to be L_0, surprisingly, the calculated κ_e of 0.45 $Wm^{-1}K^{-1}$ based on the reported σ of the PEDOT:PSS film is higher than the measured total κ. This has raised the question of the validity of the Wiedemann-Franz law or the applicability of the Sommerfeld value of L_0 for describing electronic thermal transport in conducting polymers, which are characterized by a distinctively different charge transport mechanism compared to electrons in inorganic metals. Besides polaronic conduction, the comparatively efficient intra-chain conduction compared to cross-chain conduction can result in quasi-one-dimensional (1D) conduction pathways in some conducing polymer systems. It remains unclear whether

this feature can result in a large deviation of L from L_0 or a temperature dependent L, which has been predicted theoretically for strongly interacting fermions in idealized 1D systems. [21]

The question of the validity of the Wiedemann-Franz law in conducting polymers arises not only because of the lack of theoretical understanding of the electronic thermal transport in these systems, but also because of the challenges in thermal conductivity measurements of conducting polymers, which are often prepared as thin films on insulating substrates. It is known that the transport properties of some conducting polymer thin films such as PEDOT can be highly anisotropic. PEDOT is synthesized by combining ethylenedioxythiophene (EDOT) monomers with a counterion solution typically composed of polystyrene sulfonic acid (PSS) or the smaller molecular weight Tosylate (Tos), which serve as charge balancing counterions. The layering of the PEDOT and counterion-dense regions can result in up to three orders of magnitude difference in σ between the out-of-plane and highly conducting in-plane directions.[22] While it remains a relatively straightforward practice to measure the in-plane electrical properties of a thin film on an insulating substrate, and the 3ω method and the time domain thermal reflectance technique have been established to measure the cross-plane κ of a thin film,[23, 24] measurements of the in-plane κ of these samples are difficult because of heat conduction through the substrate, radiation loss, and thermal contact resistance. Thus far, in-plane κ measurements of PEDOT thin films have relied on a modified 3ω method, which employs a variation in the heater line widths. The measurement results are fitted with a two-dimensional heat conduction model to extract an anisotropy ratio between the in-plane and the out-of-plane thermal conductivities,[12, 18] which was previously found to be between 1.1 and 1.6 for PEDOT.[13, 22] Besides the complications and uncertainties inherent in the numerical model fitting, such measurements require the deposition of a dielectric film, such as SiN_x or Al_2O_3, on top of the PEDOT film. Consequently, the PEDOT samples for thermal conductivity measurements underwent

different processing conditions compared to those for electrical conductivity measurements. Hence, accurate measurements of the transport properties along the same direction from the same conducting polymer sample are essential to better understanding the applicability of the Wiedemann-Franz law in conducting polymers, which is a fundamental question that is both timely and important for the development of organic electronic, optoelectronic, and thermoelectric materials.

In this Communication, we present a direct measurement of all three in-plane thermoelectric properties, κ, σ, and S, of the same suspended PEDOT thin films, using suspended microdevices. We find that the in-plane κ can be up to a factor 4 higher than previously measured by the 3ω method for samples supported on an insulating substrate. In addition, we find that our measured apparent Lorenz number is roughly a factor 2.5 higher than the Sommerfeld value, L_0. Phonon-assisted hopping and bipolar transport are examined as possible causes of a relatively large apparent L in this conducting polymer.

PEDOT:Tos and PEDOT:PSS thin films were prepared by either vacuum vapor phase polymerization (VVPP) or chemical polymerization (CP) (Supporting Information). The PEDOT thin film sample was transferred onto a suspended micro-device, which consists of two adjacent SiN_x membranes, each patterned with a serpentine platinum resistance thermometer (PRT), two electrodes, and six supporting beams for four-probe thermoelectric property measurements of κ, S, and σ to eliminate errors associated with contact thermal and electrical resistances. Scanning electron micrograph (SEM) images of the device are shown in **Figure 1**, and details of the measurement method are discussed in the Supporting Information and in a previous work.[25] For each sample, the sample dimensions were found from scanning electron microscopy (SEM) and atomic force microscopy (AFM) measurements following the thermoelectric measurements. Figure 1b shows the AFM measurement result for S1.

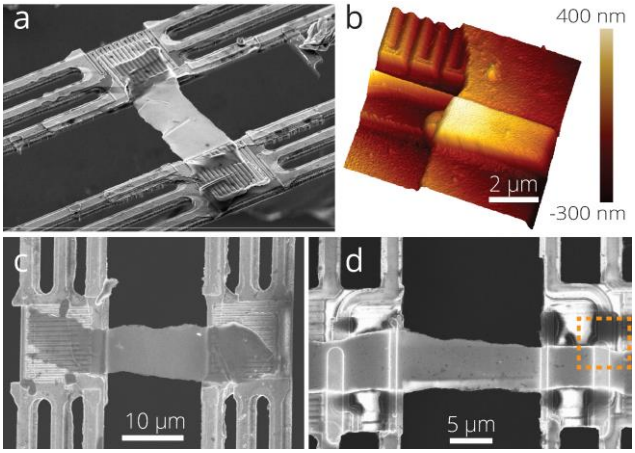

Figure 1. (a) SEM image of measurement device (S6). (b) Three-dimensional AFM map of the area of S1 outlined by the dotted orange line in (d). (c-d) SEM images of S1 and S4 on the measurement device.

For seven PEDOT:Tos samples (S1-S7) and one PEDOT:PSS (S8) sample, the measured *S* shown in **Figure 2**a is found to be positive for all samples but shows no clear correlation with σ shown in Figure 2b. The positive *S* indicates that charge is conducted by hole-type carriers, consistent with other reports on PEDOT.[12, 13] The measured *S* is linearly proportional to temperature in the temperature range studied and extrapolates to zero at 0 K, indicative of metallic conduction. In contrast, σ of most samples exhibits non-metallic behavior evident by its increase with temperature, suggestive of thermal activation of hopping conduction. One exception is S1, which shows both the highest σ and a decreasing σ with temperature at temperatures above 350 K. Highly doped polyacetylene (PA) and polyaniline (PANI) have shown a similar maximum in σ at a crossover temperature of roughly 200 K due to metallic conduction with an increasing contribution from phonon scattering at higher temperatures. Likewise, as the dopant concentration is increased in PA and PANI to obtain conductivity over 100 S/cm, the slope of σ versus *T* decreases with temperature, similar to the observed trend in all eight PEDOT samples. Moreover, σ of S1 and S2 extrapolate to non-zero

conductivity in the limit of 0 K, suggesting the presence of delocalized metallic conduction even in the absence of thermal activation.

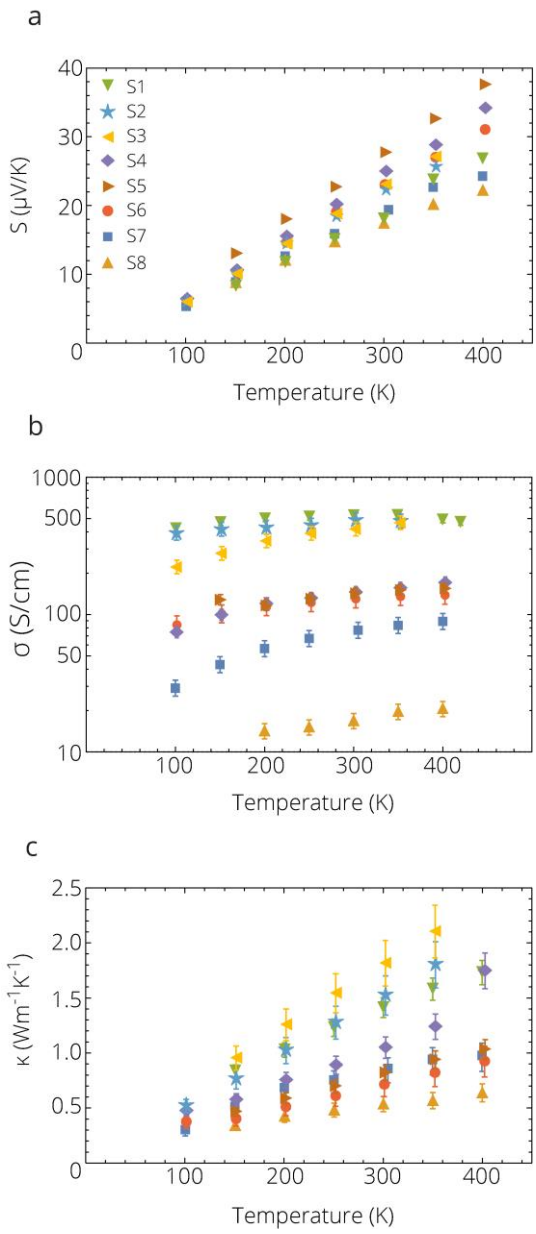

Figure 2. (a) Seebeck coefficient, (b) electrical conductivity, and (c) effective in-plane thermal conductivity with contact resistance eliminated versus temperature for the eight samples indicated in the legend of (a).

Indeed, mixed metallic S and non-metallic σ behavior of this kind is known to be characteristic of other conducting polymer systems, and has been explained by a

heterogeneous model.[26-28] Conducting polymers often possess crystalline domains with a high degree of chain alignment separated by disordered regions.[29] For example, polarized optical microscopy of PEDOT:Tos samples have shown ~20 μm semi-crystalline domains dispersed uniformly throughout the PEDOT film.[18] Furthermore, the segregation of PEDOT films into regions of excess counterion with low σ has also been observed.[18, 22] In such heterogeneous structures, electrical conduction occurs by tunneling between regions of highly conducting metallic domains separated by disordered barriers, and the measured electrical resistance and the corresponding apparent σ is largely dominated by those of the non-metallic highly resistive barrier layers [26-28] In comparison, the difference in the thermal resistance between the barrier regions and the metallic domains is not as large as the difference in the electrical resistance. As such, the temperature drop and the corresponding thermovoltage developed in the metallic domains make relatively large contributions to the measured *S*.

As shown in Figure 2c, the in-plane κ increases linearly in the temperature range studied and is a factor of 1 to 4 higher than previously reported for PEDOT:PSS and PEDOT:Tos samples of comparable electrical conductivities [12, 18] In addition to different measurement methods, it is worth noting that the measured transport properties of the suspended samples could differ from those of the samples supported on a substrate because of different processing conditions, inhomogeneity in the sample on the 10-100 μm scale, or variations in the strain. However, as the current measurement has obtained the three transport properties in the same sample and along the same direction, the results allow for a consistent investigation of the validity of the Wiedemann-Franz law in PEDOT. As shown in **Figure 3**a, in the limit of low σ, κ approaches approximately 0.5 $Wm^{-1}K^{-1}$, which represents an approximation of the lattice contribution, κ_L, to the thermal conductivity. While this value is consistent with κ_L values previously reported for low-σ PEDOT samples, the measured κ shows much clearer dependence on the measured σ than prior measurements of PEDOT

samples. Specifically, the measured κ increases with σ, by as much as a factor of three when σ is increased from 20 to about 500 S/cm. Such a pronounced increase should not be attributed alone to the variation of κ_L in different samples, and must have an electronic origin. Evidently, the same charge transport mechanism contributes to both electrical and thermal conduction, and results in an increasing contribution to κ_e with σ. In addition, the slope of the κ versus σ curves at each T provides an evaluation of the apparent Lorenz number, L, which is plotted in Figure 3b as a function of temperature. We find that the obtained apparent L is roughly a factor of 2.5 as large as the Sommerfeld value of $L_0 = \pi^2/3$, and shows no clear temperature dependence.

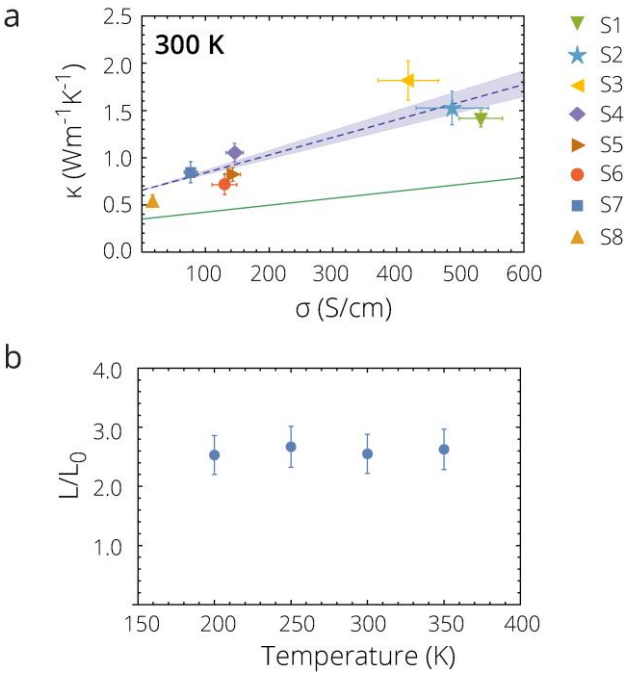

Figure 3. (a) In-plane κ versus in-plane σ for the eight samples at 300 K. Blue dotted line is a linear fit to the seven PEDOT:Tos samples, with the range of error in the slope presented as the blue shaded region. The green line is the slope predicted by the Sommerfeld value of $L_0 = \pi^2/3$. Similar plots at 200 K, 250 K, and 350 K are presented in the Supporting Information. (b) The Lorenz number found from the slope in (a) for different temperatures.

The origin of the observed deviation in the as-obtained apparent L from the Sommerfeld value is worthy of discussion as it highlights several key assumptions used in the formulation of this theoretical value based on a single parabolic band approximation. It is known that there are deviations in the value of the Lorenz number even for metals. At very low temperatures when the dominant scattering mechanism for electrons is elastic impurity scattering, the relaxation of electron momentum (charge transport) and electron energy (heat transport) are equivalent, which gives a Lorenz number very close to L_0. At temperatures above the phonon Debye temperature, which is typically around 200-300 K for common metals, electron scattering is dominated by inelastic scattering with phonons of wave vectors much greater than the Fermi wavevector of the electrons, k_F. Therefore, large-angle scattering with phonons results in a large relaxation of both momentum and energy, recovering the condition for a Lorenz number equal to L_0. However, at intermediate temperatures, in which the phonon wave vector can be small compared to the Fermi wavevector, small-angle scattering with phonons results in a greater relaxation of energy than momentum and the Lorenz number is found to decrease. In general, the Lorenz number of metals approaches $L_0(l_s/l_e)$, where l_s and l_e are the electron mean free paths for heat and charge transport, respectively. [30]

While σ of a heterogeneous conducting polymer such as PEDOT is limited by that of the non-metallic barrier layer where most of the electrical potential drop occurs, the κ_e should not be limited by this barrier layer, because the presence of parallel lattice conduction in the barrier layer facilitates heat transport between charge carriers in separated metallic domains. Nevertheless, the non-metallic barrier layer is still expected to play an important role in electronic thermal transport in PEDOT. In non-degenerate inorganic semiconductors, the Lorenz number for a single parabolic band can be reduced to $L = 5/2 + r$, where r is the exponent in the energy (E) dependence of the electron relaxation time expressed as $\tau(E) \propto E^r$.

For dominant acoustic deformation potential scattering, r = -1/2 and L takes a value of 2, whereas dominant ionized impurity scattering yields r = +3/2,[31] which can lead to L larger than L_0. As higher energy carriers are more likely to overcome the energy barrier in conducting polymers, r is expected to take a positive value,[32] giving rise to a L value larger than L_0, similar to the case of ionized impurity scattering in inorganic semiconductors. In fact, previous measurements of L in PANI thin films have shown a similarly large Lorenz number associated with the hopping conduction in low conductivity samples with localized electronic states.[33]

Furthermore, when two or more bands contribute to transport, the electrical current carried by each band does not vanish, although the total net current vanishes in the thermal conductivity measurement. The resulting Peltier heat carried by the electrons and holes leads to an additional bipolar contribution to κ_e.[34] The bipolar contribution was not included in the formulation of the Sommerfeld value for single band transport. It is known that the bipolar contribution can increase the apparent Lorenz number to be as much as a factor of 10 larger than L_0 in intrinsic Bi_2Te_3.[35, 36] Similarly, the bipolar contribution could be important in the non-metallic barrier regions of PEDOT and other conducting polymers.

In addition, while the derivation of the Sommerfeld value has assumed a non-interacting Fermi gas, a constant value for L_0 persists even in the presence of weak electron-electron interactions, as long as the system remains a metal.[37] In comparison, 1D systems with strong electron-electron interactions, such as some polymeric systems with Luttinger liquid behavior, can show a marked deviation in the value and temperature dependence of the Lorenz number.[38, 39] However, we find little evidence that our samples behave as a Luttinger liquid, as the key feature of a power law dependence of the current with voltage, $I \sim V^{\beta}$, [40] was not observed in all samples. As such, it is unlikely that the relatively large apparent L observed here can be explained by strong electron interactions as has been proposed for some other conducting polymer systems.[21]

The experimental results show that both the total thermal conductivity and the apparent Lorenz number of the suspended PEDOT samples are higher than previously reported for supported PEDOT samples, and that the electronic contribution to κ is significant. Compared to the Sommerfeld value, the relatively large apparent Lorenz number can be caused by the heterogeneous structure of the conducting polymer system, where the non-metallic barrier layer can lead to a deviation of the apparent Lorenz number from metallic to non-degenerate behavior. Specifically, both phonon-assisted hopping and a bipolar contribution in the barrier regions can increase the apparent L to be larger than L_0. These results are expected to motivate further fundamental studies of the coupling of heat and charge transport in conducting polymers as it is highly relevant to the active development of polymeric electronics, optoelectronics, and thermoelectrics.

Supporting Information

Supporting Information is available from the Wiley Online Library or from the author.

Acknowledgements

The transport measurements at Austin are supported by the US National Science Foundation Thermal Transport Processes Program (CBET-0933454). The materials synthesis efforts are supported by the European Research Council (ERC-starting-grant 307596), the Swedish foundation for strategic research (project: “Nano-material and Scalable TE materials”), the Knut and Alice Wallenberg foundation (project “Power paper”), and The Swedish Energy Agency. A.W. gratefully acknowledges the NSF Graduate Research Fellowship Program for funding. Z.U.K acknowledges the Advanced Functional Materials Center at Linköping University. The authors thank Olga Bubnova for her assistance in the sample synthesis.

Received: ((will be filled in by the editorial staff))
Revised: ((will be filled in by the editorial staff))
Published online: ((will be filled in by the editorial staff))

[1] A. J. Heeger, Angewandte Chemie International Edition 2001, 40, 2591.
[2] A. Salleo, R. J. Kline, D. M. DeLongchamp, M. L. Chabinyc, Advanced Materials 2010, 22, 3812.
[3] B. J. de Gans, P. C. Duineveld, U. S. Schubert, Advanced Materials 2004, 16, 203.
[4] H. Shirakawa, E. J. Louis, A. G. MacDiarmid, C. K. Chiang, A. J. Heeger, Journal of the Chemical Society, Chemical Communications 1977, 578.
[5] J. H. Burroughes, D. D. C. Bradley, A. R. Brown, R. N. Marks, K. Mackay, R. H. Friend, P. L. Burns, A. B. Holmes, Nature 1990, 347, 539.
[6] Z. Bao, A. Dodabalapur, A. J. Lovinger, Applied Physics Letters 1996, 69, 4108.
[7] Y. Yang, J. Ouyang, L. Ma, R. J. H. Tseng, C. W. Chu, Advanced Functional Materials 2006, 16, 1001.
[8] G. Li, R. Zhu, Y. Yang, Nat Photon 2012, 6, 153.
[9] Y. Li, W. Zhou, H. Wang, L. Xie, Y. Liang, F. Wei, J.-C. Idrobo, S. J. Pennycook, H. Dai, Nat Nano 2012, 7, 394.
[10] M. He, F. Qiu, Z. Lin, Energy & Environmental Science 2013, 6, 1352.
[11] D. G. Cahill, P. V. Braun, G. Chen, D. R. Clarke, S. Fan, K. E. Goodson, P. Keblinski, W. P. King, G. D. Mahan, A. Majumdar, H. J. Maris, S. R. Phillpot, E. Pop, L. Shi, Applied Physics Reviews 2014, 1.
[12] G.-H. Kim, L. Shao, K. Zhang, K. P. Pipe, Nature Materials 2013, 12, 719
[13] O. Bubnova, Z. U. Khan, H. Wang, S. Braun, D. R. Evans, M. Fabretto, P. Hojati-Talemi, D. Dagnelund, J.-B. Arlin, S. D. Yves H. Geerts, D. W. Breiby, J. W. Andreasen, R. Lazzaroni, W. M. Chen, I. Zozoulenko, M. Fahlman, P. J. Murphy, M. Berggren, X. Crispin, Nature materials 2014, 13, 190.
[14] D. Kim, Y. Kim, K. Choi, J. C. Grunlan, C. Yu, ACS Nano 2009, 4, 513.
[15] C. Meng, C. Liu, S. Fan, Advanced Materials 2010, 22, 535.
[16] B. Zhang, J. Sun, H. E. Katz, F. Fang, R. L. Opila, ACS Applied Materials & Interfaces 2010, 2, 3170.
[17] C. Liu, B. Lu, J. Yan, J. Xu, R. Yue, Z. Zhu, S. Zhou, X. Hu, Z. Zhang, P. Chen, Synthetic Metals 2010, 160, 2481.
[18] O. Bubnova, Z. U. Khan, A. Malti, S. Braun, M. Fahlman, M. Berggren, X. Crispin, Nature Materials 2011, 10, 429
[19] H. S. a. S. Scherrer, *CRC Handbook of Thermoelectrics, Chapter 19*, CRC Press, 1995.
[20] G. S. Kumar, G. Prasad, R. O. Pohl, J Mater Sci 1993, 28, 4261.
[21] A. N. Aleshin, H. J. Lee, Y. W. Park, K. Akagi, Physical Review Letters 2004, 93, 196601.
[22] A. M. Nardes, M. Kemerink, R. A. J. Janssen, J. A. M. Bastiaansen, N. M. M. Kiggen, B. M. W. Langeveld, A. J. J. M. van Breemen, M. M. de Kok, Advanced Materials 2007, 19, 1196.
[23] D. G. Cahill, Review of Scientific Instruments 1990, 61, 802.
[24] D. G. Cahill, Review of Scientific Instruments 2004, 75, 5119.
[25] A. Mavrokefalos, M. T. Pettes, F. Zhou, L. Shi, Review of Scientific Instruments 2007, 78.
[26] A. B. Kaiser, Advanced Materials 2001, 13, 927.
[27] A. N. Aleshin, S. R. Williams, A. J. Heeger, Synthetic Metals 1998, 94, 173.
[28] P. Sheng, Physical Review B 1980, 21, 2180.
[29] P. J. Phillips, Reports on Progress in Physics 1990, 53, 549.
[30] T. M. Tritt, *Thermal Conductivity: Theory, Properties, and Applications*, Kluwer Academic / Plenum Publishers, New York 2004.

[31] K. Seeger, *Semiconductor Physics: An Introduction*, Springer, Berlin 1997.
[32] E. Gorham-Bergeron, D. Emin, Physical Review B 1977, 15, 3667.
[33] H. Yoon, B. S. Jung, H. Lee, Synthetic Metals 1991, 41, 699.
[34] H. J. Goldsmid, *Introduction to Thermoelectricity*, Springer Series in Material Science, New York 2010.
[35] M. T. Pettes, J. Maassen, I. Jo, M. S. Lundstrom, L. Shi, Nano Letters 2013, 13, 5316.
[36] B.-L. Huang, M. Kaviany, Physical Review B 2008, 77, 125209.
[37] C. Castellani, C. DiCastro, G. Kotliar, P. A. Lee, G. Strinati, Physical Review Letters 1987, 59, 477.
[38] C. L. Kane, M. P. A. Fisher, Physical Review Letters 1996, 76, 3192.
[39] M. R. Li, E. Orignac, EPL (Europhysics Letters) 2002, 60, 432.
[40] J. Voit, Reports on Progress in Physics 1995, 58, 977.

Supporting Information

Significant electronic thermal transport in the conducting polymer poly(3,4-ethylenedioxythiophene) (PEDOT) Supporting Information

*Annie Weathers, Zia Ullah Khan, Robert Brooke, Drew Evans, Michael T. Pettes, Xavier Crispin, and Li Shi**

A. Weathers, M. T. Pettes Prof. L. Shi
Department of Mechanical Engineering, The University of Texas at Austin, Austin, 78712,USA
E-mail: lishi@mail.utexas.edu

Z.U. Khan, Prof. X. Crispin
Linkoping University, Department of Science and Technology, Organic Electronics, SE-601 74 Norrkoping, Sweden

R. Brooke, Dr. D. Evans
Thin Film Coatings Group, Mawson Institute, University of South Australia, Mawson Lakes, 5095, Australia

1. Synthesis of PEDOT thin films

In the case of the vacuum vapor phase polymerization (VVPP) samples, a mixture of 40 wt% Fe-Tosylate in butanol (Clevios CB 40), the triblock copolymer poly(ethylene glycol-propylene glycol-ethylene glycol) (Mw = 5800 from Sigma Aldrich), and ethanol was spin coated on a glass substrate and exposed to ethylenedioxythiophene (EDOT) vapor in vacuum and cleaned in ethanol.[1] During the ethanol cleaning step, the PEDOT:Tos was made free standing,[2] and suspended on perforated aluminum substrates, rendering the area of the VVPP PEDOT:Tos permanently free standing. Chemically polymerized (CP) PEDOT:Tos samples were prepared from a mixture of EDOT monomer, Fe-Tosylate solution, and pyridine (Sigma Aldrich), which were spin coated on a glass or Si substrate and baked on a hot plate at 100 ˚C for five minutes and cleaned in butanol and water.[3] PEDOT:PSS films were prepared by adding 5 wt% dimethyl sulfoxide (DMSO) to a mixture of PEDOT:PSS suspension (Clevios

PH1000) and 1.2 wt% silquest (Sigma Aldrich). This material was spin coated on a glass substrate and baked on a hot plate at 120 ˚C for 5 minutes. In this and previous works on chemically polymerized PEDOT:Tos,[4] the polymerization of the EDOT:Tos mixture occurs after spin-coating, and therefore no polymer chains exist during spin coating. As such, the anisotropy in the transport properties is expected to be less than if polymerization occurs before spin-coating.[4] Similarly, anisotropy in the VVPP PEDOT:Tos may arise from the structure directing behavior of the triblock copolymer additive in the oxidant solution, as again, polymerization occurs after spin coating.

2. Sample Fabrication

As illustrated in **Figure S1**, two sample fabrication methods were utilized to minimize the modification of the properties of the films by the processing conditions. First, the spun films were scraped with a razor blade and exfoliated for chemically polymerized (CP) samples or removed from the perforated aluminum substrate with tweezers for vacuum vapor phase polymerization (VVPP) samples, and placed onto either a (i) poly-methyl methacrylate (PMMA)/polyvinyl alcohol (PVA) bilayer film on a Si substrate or (ii) directly onto a clean Si substrate. In method (i), the PMMA layer carrying the PEDOT sample was released from the substrate by dissolving the PVA in water, and the PMMA layer was positioned with the help of a home-built micromanipulator on the suspended micro-device. The PMMA layer was dissolved by placing the entire device into acetone, which leaves only the sample suspended across the measurement device. In method (ii), 8% PVA solution was drop cast onto the Si substrate containing the PEDOT films and baked at 80 ˚C for 1 minute.[5] The PVA was peeled from the Si substrate with tweezers, releasing the PEDOT films. The PVA film was positioned on the measurement device so that the sample bridged the two membranes, and the PVA was dissolved by submerging the entire device in water. The PEDOT films were found in a separate test to be stable in acetone for at least 30 minutes, and in water for a period of many hours.

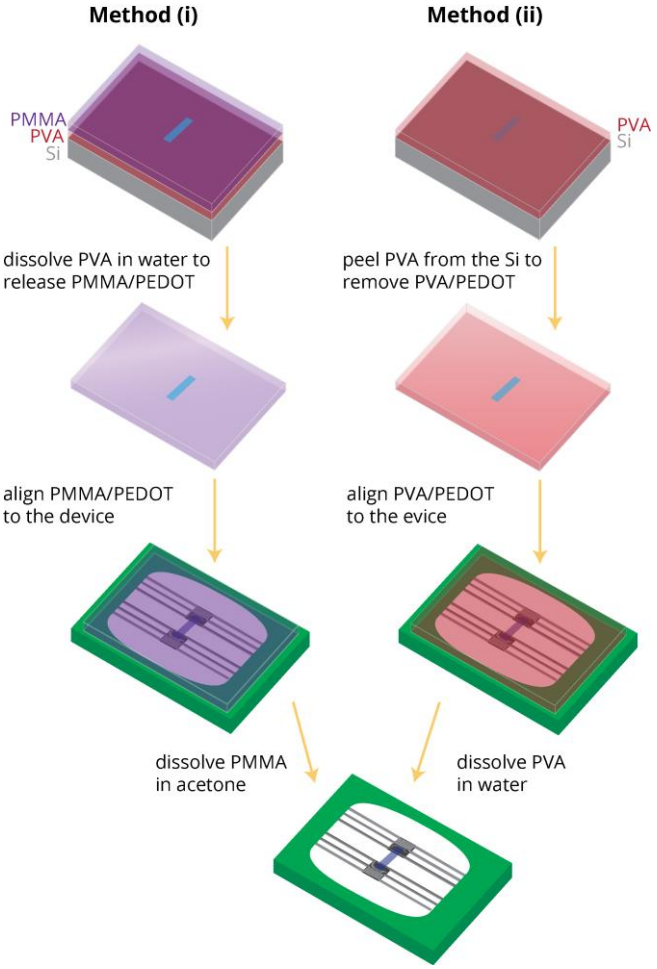

Figure S1. Procedure for sample fabrication. A PEDOT film is exfoliated onto either (i) a PMMA(purple)/PVA(red) bilayer on Si(gray) or (ii) a clean Si substrate on which a PVA layer is drop casted. Either (i) the PVA is dissolved in water and the PMMA/ PEDOT film is released or (ii) the PVA/ PEDOT film is peeled from the Si. The PMMA or PVA carrier layer is placed on top of the measurement device and the sample is aligned to the electrodes. The carrier layer is dissolved in either acetone or water, leaving only the PEDOT film on the measurement device.

3. Thermoelectric Measurements

In brief, the thermal measurement technique is based on a steady state comparative method, in which the measured temperature drop across the sample is compared to the temperature drop across the supporting SiN_x beams, which is used to obtain the thermal resistance and *S* of the suspended sample. Separate four-probe electrical measurements are

used to obtain σ under the same vacuum environment along the same transport direction. The obtained sample thermal resistance contains a contribution from the contact thermal resistance between the sample and the two serpentine Pt resistance thermometers (PRTs). A four-probe thermoelectric measurement method was employed to determine the contact thermal resistance.[6] The obtained sample thermal resistance contains a contribution from contact thermal resistance between the sample and the two PRTs. A four-probe thermoelectric measurement method was employed to determine the contact thermal resistance.[6] In this method, the thermovoltages between the two inner electrodes and between the two outer electrodes are measured simultaneously together with the thermal conductance measurement. The ratio between the two measured thermovoltages is used to determine the temperature drop at the contacts and the thermal contact resistance between the sample and PRTs.[6] Such four-probe thermoelectric measurements yield both the intrinsic thermal conductance and Seebeck coefficient of the suspended sample.

Furthermore, as contact thermal resistance will tend to underestimate the thermal conductivity, so too will radiation loss from the surface of the sample. All samples studied here have been found to have an error of less than 1 % associated with neglecting radiation loss from the sample surface.[7] In comparison, heat transfer via radiation and residual gas molecules in the evacuated sample space can lead to an overestimation of the sample thermal conductivity by less than 3%, based on separate thermal measurements of a blank device without a sample bridging the two PRTs.

4. Microdevice Fabrication

The four-probe thermoelectric property measurement is based on the assumption of a uniform temperature in each membrane, which is valid when the thermal resistance values of the suspended sample and the supporting beams are orders of magnitude larger than the internal thermal resistance in the membrane. [8-10] While this condition is still satisfied by the low-thermal conductivity PEDOT samples measured in this work, a modified device design

was fabricated to further reduce the membrane thermal resistance. In the previous design, referred as Design A, the two Pt electrodes are placed on the inside edge of the SiN_x membrane and next to the PRT, as shown in **Figure S2**a with false coloring of the electrodes, serpentine, and sample. For the four samples measured with the original design, an additional Au layer was evaporated through the open window of a SiN_x shadow mask on the four contact areas, as shown in Figure 1d. Following shadow-mask deposition, the thermal contact resistance determined from the temperature drop at the contacts is in the range between 5% and 15% of the total measured thermal resistance. In the new design, referred as Design B, shown in Figure S2b, the PRT covers nearly the entire SiN_x membrane of a reduced lateral dimension compared to Design A, and two Pd electrodes are placed on top of a 80-nm-thick HfO_2 film deposited on the PRTs. Because of the increase in the coverage of the membrane by Pt and Pd, which has relatively high thermal conductivity, the internal membrane thermal resistance is further decreased. Consequently, the contact temperature drop and contact thermal resistance determined from the two measured thermovoltages for the five samples measured by this new design are negligible, even when no additional metal was evaporated on the contact areas of these two samples. Furthermore, for Design B, electrical contact was established between the transferred organic film and the underlying Pd electrodes on the SiN_x membranes without the use of shadow-mask evaporation of Au on the contacts.

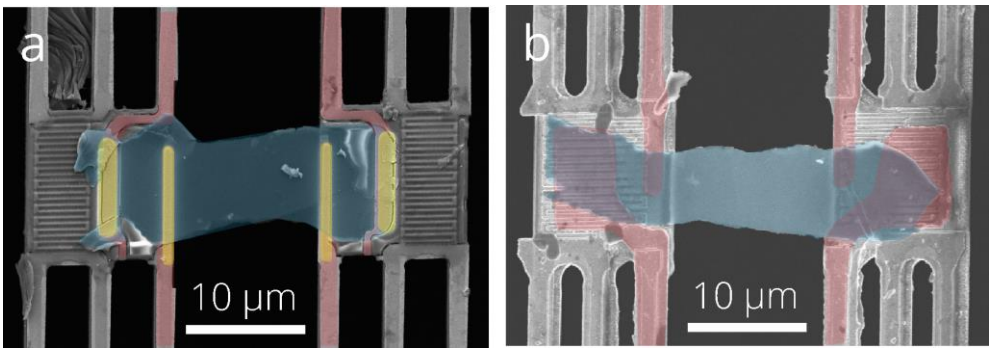

Figure S2. (a) Design A and (b) Design B with false coloring of the electrodes (red), sample (blue), and Au shadow-mask deposition (yellow).

The three measurement samples (S1, S7, S8) based on Design A contain one or two 500 nm wide SiN_x bars, which connect the two suspended membranes and provides structural support during the sample transfer process. In Figure 1d, the bar is visible supporting the bottom edge of the sample. To remove the contribution to the measured thermal conductance from the supporting bar, the PEDOT sample in S7 was removed with O_2 plasma after thermoelectric measurements, and the thermal conductance of only the supporting bars, G_{bar}, was measured. Likewise, the thermal conductance of the SiN_x bars for other devices was calculated assuming the same $G_{bar}L$ as for S7. The conductance of the SiN_x bar was subtracted from the total thermal conductance measured with the sample. Typically the supporting bar contributes 50% to the total measured thermal conductance. The connecting bars were not present for the other five samples.

Table 1 lists the sample type, dimensions, device design, carrier layer in fabrication process, shadow-mask deposition, and number of supporting bars for each of the eight samples measured.

Table 1. Summary of sample fabrication and dimensions

Symbol		Sample Type	Dimensions			Device Type	Carrier Layer	# of bars
			w (μm)	L (μm)	t (nm)			
▼	S1	VVPP PEDOT:Tos	5.9 ± 0.3	15.0 ± 0.1	167 ± 5	A	PMMA	1
★	S2	VVPP PEDOT:Tos	5.8 ± 0.5	15.6 ± 0.2	130 ± 10	B	PVA	0
◄	S3	VVPPP PEDOT:Tos	6.0 ± 0.5	12.0 ± 0.2	130 ± 10	B	PVA	0
♦	S4	CP PEDOT:Tos	6.4 ± 0.3	13.6 ± 0.3	135 ± 10	B	PMMA	0
►	S5	CP PEDOT:Tos	8.5 ± 0.3	14.2 ± 0.1	130 ± 10	B	PMMA	0
●	S6	CP PEDOT:Tos	6.9 ± 0.6	14.4 ± 0.4	167 ± 5	B	PMMA	0
■	S7	VVPP PEDOT:Tos	8.7 ± 0.3	14.4 ± 0.6	165 ± 20	A	PMMA	2
▲	S8	CP PEDOT:PSS	10.4 ± 0.5	10.4 ± 0.5	230 ± 10	A	PMMA	1

5. Lorenz Number Calculation

The slope of the κ versus σ plot at each T provides an evaluation of the apparent Lorenz number, L. **Figure S3** shows the plot of κ versus σ at 200 K, 250 K, and 350 K, while Figure 3 in the main text displays the data at 300 K. The uncertainties in the apparent L are determined by considering the individual uncertainties of κ and σ at each data point in the linear fit.[11]

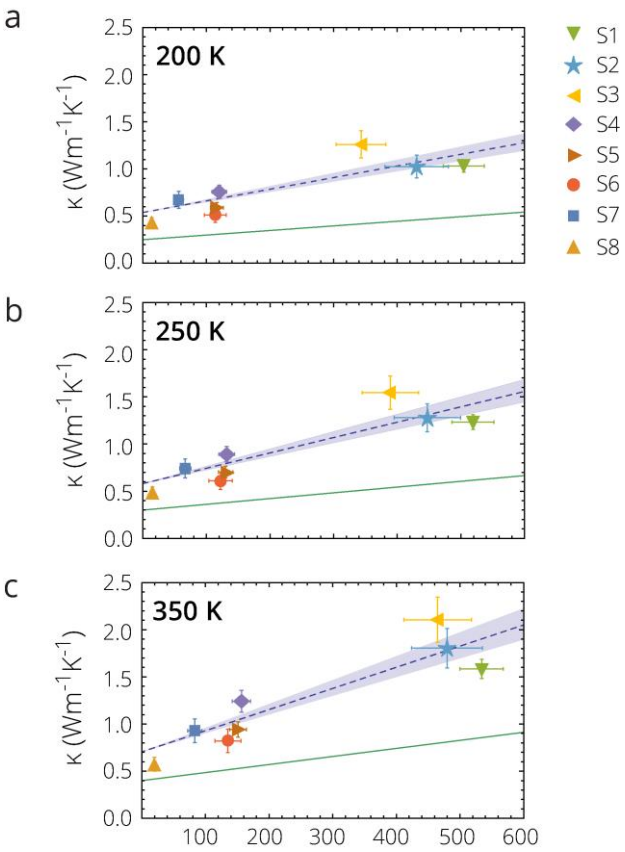

Figure S3. (a-c) In-plane κ versus in-plane σ for the eight samples at 200 K., 250 K, and 350 K. Blue dotted line is a linear fit to the seven PEDOT:Tos samples, with the range of error in the slope presented as the blue shaded region. The green line is the slope predicted by the Sommerfeld value of $L_0 = \pi^2/3$. A similar plot at 300 K is presented in Figure 3 of the main text.

[1] M. V. Fabretto, D. R. Evans, M. Mueller, K. Zuber, P. Hojati-Talemi, R. D. Short, G. G. Wallace, P. J. Murphy, Chemistry of Materials 2012, 24, 3998.
[2] N. Vucaj, M. D. J. Quinn, C. Baechler, S. M. Notley, P. Cottis, P. Hojati-Talemi, M. V. Fabretto, G. G. Wallace, P. J. Murphy, D. R. Evans, Chemistry of Materials 2014, 26, 4207.
[3] B. Winther-Jensen, K. West, Macromolecules 2004, 37, 4538.
[4] O. Bubnova, Z. U. Khan, A. Malti, S. Braun, M. Fahlman, M. Berggren, X. Crispin, Nature Materials 2011, 10, 429
[5] F. Greco, A. Zucca, S. Taccola, A. Menciassi, T. Fujie, H. Haniuda, S. Takeoka, P. Dario, V. Mattoli, Soft Matter 2011, 7, 10642.
[6] A. Mavrokefalos, M. T. Pettes, F. Zhou, L. Shi, Review of Scientific Instruments 2007, 78.
[7] K. Bi, A. Weathers, S. Matsushita, M. T. Pettes, M. Goh, K. Akagi, L. Shi, Journal of Applied Physics 2013, 114.
[8] A. L. Moore, L. Shi, Measurement Science and Technology 2011, 22, 015103.
[9] I. Jo, M. T. Pettes, E. Ou, W. Wu, L. Shi, Applied Physics Letters 2014, 104.
[10] J. Wang, L. Zhu, J. Chen, B. Li, J. T. L. Thong, Advanced Materials 2013, 25, 6884.
[11] K. K. Brown, H. W. Coleman, W. G. Steele, Journal of Fluids Engineering 1998, 120, 445.